agriculture

MDPI

Article

Cattle-Manure Nitrogen Substitution Restores the Carbon and Nitrogen Pools of Degraded Black Soil Under Maize Monoculture: A 13-Year Equal-Nitrogen Field Experiment

Liyan Wang, Xuexue Jiao, Ding Li, Fenglin Zhang, Bin Wang and Hongbin Wang *

College of Resource and Environmental Science, Jilin Agricultural University, Changchun 130118, China
* Correspondence: asionwang@163.com

Abstract

Long-term sole chemical nitrogen fertilization induces severe degradation of Northeast Chinese black soil (Mollisols), yet few long-term field studies have disentangled how gradient cattle manure nitrogen substitution modulates soil carbon and nitrogen pools. We hypothesized that, under equal nitrogen input, organic nitrogen substitution simultaneously restores degraded black soil carbon and nitrogen and sustains maize productivity through improved aggregate physical protection and divergent carbon pool accumulation. In an ongoing 13-year equal nitrogen field experiment (five treatments: N0, M0, M25, M50, M100), soil carbon fractions, water-stable aggregates, carbon mineralization kinetics, multi-component nitrogen across 0–40 cm and maize yield were measured post-harvest of the 13th season, with structural equation modeling applied. Compared with sole chemical fertilization (M0), organic substitution increased 0–20 cm soil organic carbon storage by 24.32–37.84%, total nitrogen storage by 14.29–32.65%, the proportion of >2 mm macroaggregates by 80.00–225.00% and aggregate mean weight diameter by up to 63.53%, while raising the ammonium nitrogen proportion by 59.12–169.23% and reducing the nitrate nitrogen proportion by up to 50.32%. M50 maximized labile carbon fractions and maize yield, whereas M100 accumulated stable carbon fractions and nitrogen storage without yield penalty. Gradient manure nitrogen substitution restores degraded black soil carbon and nitrogen and sustains maize productivity, with moderate substitution favoring short-term nutrient supply and yield and full substitution delivering long-term carbon sequestration and nitrogen retention.

Keywords: black soil; degradation; organic–inorganic nitrogen gradient substitution; soil carbon pool; nitrogen component; carbon sequestration; nitrogen storage stability

Check for updates

Academic Editor: Guisheng Zhou

Received: 26 September 2026
Revised: 9 November 2026
Accepted: 12 November 2026
Published: 18 November 2026

Copyright: © 2026 by the authors. Licensee MDPI, Basel, Switzerland. This article is an open access article distributed under the terms and conditions of the Creative Commons Attribution (CC BY) license.

1. Introduction

Northeast black soil is a precious agricultural soil resource in China and a core production area for ensuring national food security [1–3]. Long-term high-intensity cultivation and unreasonable nutrient management have led to increasingly severe degradation of black soil in Northeast China, manifested as intensified soil erosion, thinning of the black soil layer and continuous decline in organic matter content [4–6]; monitoring data show that the average annual loss thickness of the black soil surface can reach 0.3–1.0 cm, and the SOC content of farmland in the central region has decreased by 9.06% compared with 2002 [7–9]. The decline of the black soil carbon pool has become a key bottleneck restricting the sustainable development of regional agriculture [10].

The widespread application of chemical fertilizers has greatly promoted crop production, but long-term single and excessive use of chemical fertilizers has triggered a series of ecological problems, including low fertilizer use efficiency, soil acidification, compaction, nitrogen leaching, greenhouse gas emissions and farmland non-point source pollution [11–13]. Organic fertilizers, with their comprehensive nutrients and dual functions of improving soil and enhancing soil fertility, can sustainably supplement carbon sources and nutrients, and the combined application of organic and inorganic fertilizers can avoid the drawbacks of applying either alone [14–20]. Nevertheless, because pure organic fertilization releases nutrients slowly and may cause yield reduction, the partial substitution of chemical fertilizers with organic fertilizers has become the mainstream direction of farmland nutrient management and a key technical path for black soil conservation and green agricultural development.

Soil organic carbon fractions differ in turnover rate and stability and respond differentially to agronomic measures, and aggregate physical protection is a key factor maintaining the long-term stability of the carbon pool [21–26]. Although organic–inorganic combined fertilization has been extensively studied, three major knowledge gaps remain under long-term equal nitrogen field conditions: (1) how gradient cattle manure nitrogen substitution drives divergent responses of active versus stable carbon pools; (2) how aggregate physical protection, organic carbon mineralization turnover and multi-form nitrogen transformation couple along soil profiles; and (3) how different organic substitution ratios trade off soil carbon–nitrogen restoration against maize productivity. This study was therefore conducted on an ongoing long-term field experiment initiated in 2012 in Gongzhuling City, Jilin Province, with soil sampling and laboratory analyses carried out in October 2025 after 13 consecutive maize growing seasons; five equal nitrogen treatments (N0, M0, M25, M50, M100) were compared for soil carbon fractions, aggregate composition, carbon mineralization kinetics, multi-component nitrogen across 0–40 cm and maize yield, with structural equation modeling (SEM) applied to reveal the coupling among indicators. Hypothesis: Under equal nitrogen input, organic manure nitrogen substitution simultaneously restores the carbon and nitrogen pools of degraded black soil and sustains maize productivity through improved aggregate physical protection and divergent carbon pool accumulation, and the trade-off between short-term nutrient supply and long-term carbon sequestration is determined by the substitution ratio.

2. Materials and Methods

2.1. Basic Information of the Experimental Area

The experimental site is located in Chaoyangpo Town, Gongzhuling City, Jilin Province, China (43°36′ N, 124°43′ E), with a semi-humid continental monsoon climate in the northern temperate zone, four distinct seasons, and simultaneous rainfall and heat. The main climatic indices of the site, presented against the backdrop of long-term averages, are summarized in Table 1; the daily average temperature, precipitation and sunshine duration data during the research period were sourced from the Gongzhuling National Meteorological Observatory of the China Meteorological Administration.

The soil type is typical degraded black soil (Mollisols) that had been depleted by long-term intensive maize monoculture before the experiment. The topsoil textural class was a medium loam (clay content approximately 280 g kg^{-1}), the parent material was Quaternary loess-like deposits, and the depth of the humus layer was approximately 30 cm (thin-layer black soil); the natural (undisturbed) soil organic carbon content of the same soil type under native grassland was 23.6 g kg^{-1}, and the soil had been under continuous agricultural cultivation for approximately 40 years before the experiment. The physicochemical properties of the 0–20 cm topsoil at the start of the experiment (2012) were as follows: pH

value 5.6; soil organic matter content 19.4 g kg^{-1}; total nitrogen content 1.033 g kg^{-1}; total phosphorus content 1.03 g kg^{-1}; soil bulk density 1.28 g cm^{-3}. These initial values, markedly lower than those of undegraded Mollisols in the region, evidenced the degraded condition of the soil at the outset, and in this study stratified sampling was conducted at 0–20 cm and 20–40 cm. The field long-term positioning experiment was initiated in 2012, with maize planted as the test crop; maize was sown in late April (25–30 April) and harvested in early October (1–5 October) each year, and the maize variety was Zhengdan 958. Cow manure was selected as the organic fertilizer for the substitution treatment. During the experimental period (May–September), the daily average temperature was 17–25 °C, the daily average sunshine duration was 8.3–9.5 h, and the total precipitation was about 480–510 mm, concentrated in July and August (more than 65% of the total precipitation during the growth period); there was no extreme high temperature, low temperature, freezing damage or continuous rainstorm disaster, and the meteorological conditions were generally suitable for maize growth.

Table 1. Climate characteristics of the experimental site (long-term averages and values during the experimental period).

Climatic Index	Long-Term Average	During Experimental Period (2012–2025)
Annual mean air temperature (°C)	5.5	6.1
Extreme maximum air temperature (°C)	38.2	38.6
Extreme minimum air temperature (°C)	−35.7	−33.8
Annual sunshine duration (h)	2689.4	2584.6
Sunshine duration in growing season (May–Sep, h)	1286.3	1236.4
Total solar radiation (kcal cm^{-2})	126.43	124.86
Photosynthetically active radiation (kcal cm^{-2})	62.31	61.24
Accumulated temperature ≥ 0 °C (°C d)	3185.2	3312.5
Accumulated temperature ≥ 10 °C (°C d)	2968.7	3046.8
Frost-free period (d)	145–150	148–156
Mean daily air temperature in growing season (°C)	16.3–24.2	17–25
Mean daily sunshine duration in growing season (h)	8.5–9.2	8.3–9.5
Total precipitation in growing season (mm)	470–530	480–510 (July–August > 65%)

2.2. Experimental Design

In 2012, a long-term fixed-position field experiment was established and remains ongoing. Soil sampling and laboratory analyses for this study were completed in October 2025 after 13 consecutive maize growing seasons. Five equal nitrogen fertilization treatments were set up: no fertilization (N0), sole chemical fertilizer application (M0), and 25% (M25), 50% (M50) and 100% (M100) organic manure nitrogen substitution. The trial adopted a fully randomized block design with three replications, each plot covering 54 m^2. The tested crop was maize (*Zea mays* L.). The textural class and the clay content of the topsoil of the experimental field, which are relevant to humus binding, are provided in Section 2.1. The applied chemical fertilizers included urea (N 46%), diammonium phosphate (N 18%, P_2O_5 46%) and potassium chloride (K_2O 60%), and the organic fertilizer was cattle manure (N 1.35%, P_2O_5 1.09%, K_2O 1.15%). All treatments maintained an equal total nitrogen input of 180 kg N ha^{-1}; the nitrogen supplied by diammonium phosphate was included in this total, i.e., the chemical N portion was jointly supplied by urea and diammonium phosphate, and the cattle manure N and chemical N together constituted the 180 kg N ha^{-1} quota in each fertilized treatment (M0, M25, M50 and M100). The specific nitrogen application rates and substitution amounts of each treatment are listed in Table 2. Cattle manure, phosphate fertilizer and potassium fertilizer were applied once as a base fertilizer in spring before

ridging; one third of the chemical nitrogen fertilizer was applied as a base fertilizer in the spring before ridging, and the remaining two thirds were topdressed at the maize jointing stage. Phosphorus and potassium were supplemented by chemical fertilizers so that P_2O_5 and K_2O inputs were equal across all treatments after accounting for the phosphorus and potassium supplied by cattle manure.

Table 2. Fertilizer application rates and nitrogen substitution amount under different fertilization treatments.

Treatment	Total N Input (kg N ha^{-1})	Manure-Derived N (kg N ha^{-1})	Chemical-Derived N (kg N ha^{-1})	N Substitution Ratio (%)
N0	0	0	0	0
M0	180	0	180	0
M25	180	45	135	25
M50	180	90	90	50
M100	180	180	0	100

Stratified soil samples were collected in October 2025, i.e., after the 13th consecutive maize growing season at the post-harvest stage, from two soil layers of 0–20 cm and 20–40 cm. All soil samples analyzed in the present study were obtained from this single post-harvest sampling campaign for the determination of soil carbon fractions, water-stable aggregate composition, carbon mineralization kinetics, soil nitrogen components and related indicators. After sampling, soil samples were loaded into labeled self-sealing bags and transported back to the laboratory under low-temperature conditions. Undecomposed plant residues and gravel were manually removed, and fresh subsamples were quickly sieved through a 2 mm sieve. A portion of these fresh soil samples were sealed and stored at 4 °C in the dark and analyzed within two weeks for labile indicators, including inorganic nitrogen; the remaining soil samples were naturally air-dried, sieved and preserved for subsequent index measurement. Consistent field management was conducted across all plots throughout the maize growing season. Manual weeding was performed regularly to eliminate weeds. Integrated pest management was carried out targeting maize diseases and insect pests, physical and biological control methods were prioritized, and low-toxicity chemical pesticides were supplemented only when pest pressure reached the control threshold. Timely seedling watering was conducted if soil moisture was insufficient after sowing; drip irrigation was adopted to replenish water when there was no effective rainfall for 15 consecutive days. Drainage ditches were cleaned periodically during rainy seasons to drain accumulated water and prevent field waterlogging.

2.2.1. Maize Yield

During the mature stage of the maize, representative areas with uniform growth were selected in each treatment zone to define a 10 m^2 yield test plot. Maize was planted at a density of 60,000 plants ha^{-1}, and the planting configuration was uniform 60 cm rows with 28 cm within-row spacing (60 cm × 28 cm). All maize ears in the plot were manually harvested, and the ears were naturally air-dried to a constant weight before being threshed. The grain moisture content was measured using a grain moisture analyzer, and was converted to the maize grain yield under 14% standard moisture content conditions, with the unit of kg ha^{-1}. Because yield was estimated on representative 10 m^2 subplots rather than the whole plot, the reported grain yield reflects the plot mean at the measured plant density, and three replicate plots per treatment were used to account for field variability.

Three biological replicates were set for each treatment, and yield composition indicators such as grain number per ear and thousand grain weight were synchronously calculated.

2.2.2. Organic Carbon Content and Organic Carbon Storage

Soil organic carbon (SOC) content was determined by the potassium dichromate external heating oxidation method: an air-dried soil sample passing through a 0.15 mm sieve was oxidized by a potassium dichromate–concentrated sulfuric acid solution at a high temperature, and the SOC content (g kg^{-1}) was calculated by titration with a standard ferrous sulfate solution. The soil bulk density was determined for each layer, and SOC storage (kg m^{-2}) was calculated layer by layer and summed to obtain the total SOC storage of the 0–40 cm soil profile.

2.2.3. Soil Active Carbon Component

Easily oxidizable organic carbon was determined by the potassium permanganate oxidation method [27]: an air-dried soil sample sieved through a 0.25 mm sieve was oxidized with potassium permanganate solution, and after constant temperature oscillation, centrifugation and dilution of the supernatant, the easily oxidizable organic carbon content was measured colorimetrically at 565 nm. Microbial biomass carbon was determined by the chloroform fumigation–extraction method [28]: fresh soil sieved through a 2 mm sieve was divided into fumigated and non-fumigated subsamples, extracted with potassium sulfate solution, and the extracts were analyzed with a total organic carbon analyzer. Soluble organic carbon was determined according to [29]: fresh soil sieved through a 2 mm sieve was shaken with deionized water at a soil-to-water ratio of 1:4 at 25 °C for 30 min, and the filtrate obtained after high-speed centrifugation was measured with a total organic carbon analyzer. Particulate organic carbon was determined by dispersing air-dried soil with sodium hexametaphosphate solution, sieving, collecting the organic matter retained on the sieve, and analyzing its organic carbon content by the potassium dichromate external heating method [30].

2.2.4. Stable Organic Carbon Component

Heavy fraction organic carbon was separated by the density fractionation method [31]: air-dried soil sieved through a 2 mm sieve was dispersed in a sodium iodide heavy liquid, the suspended light fraction was removed by centrifugation after constant temperature oscillation, and the residual sediment was washed repeatedly with deionized water, dried, ground and analyzed for organic carbon by the potassium dichromate external heating method. Mineral-bound organic carbon was determined by the potassium dichromate external heating oxidation method on the soil residue obtained after removal of particulate organic matter and ground through a 0.15 mm sieve. Stubborn (recalcitrant) organic carbon was determined by acid hydrolysis: soil samples were refluxed with 6 mol L^{-1} hydrochloric acid at a high temperature, and the washed, dried and ground hydrolysis residue was analyzed for organic carbon content.

2.2.5. Humus Carbon Components

Humus carbon fractions were determined according to the humus grouping extraction method [30]. An air-dried soil sample sieved through a 0.25 mm sieve was extracted with a mixed solution of 0.1 mol L^{-1} NaOH and 0.1 mol L^{-1} $Na_4P_2O_7$ by constant temperature oscillation, and the humic acid-containing extract and humin residue were separated by centrifugation. The pH of the extract was adjusted to 1.0 with hydrochloric acid, and after settling and centrifugation, humic acid (precipitate) and fulvic acid (supernatant) were obtained; the humic acid precipitate was washed and re-dissolved to volume, and the fulvic

acid supernatant was directly diluted. The humin residue was washed, dried and ground. The organic carbon contents of humic acid, fulvic acid and humin were determined by the potassium dichromate external heating method.

2.2.6. Soil Aggregate Composition and Aggregate Stability Parameters

Water-stable aggregates were determined by the Yoder wet-sieving method. Air-dried soil, after the removal of plant residues and gravel, was placed on a set of sieves with pore sizes of 2 mm, 0.25 mm and 0.053 mm, immersed in deionized water, and wet-sieved at an amplitude of 3 cm and a frequency of 30 times per minute for 15 min. Aggregates retained on each sieve (>2 mm, 0.25–2 mm and 0.053–0.25 mm) were collected separately, oven-dried at 60 °C to constant weight and weighed. The distribution ratios of water-stable aggregates of different particle sizes were calculated from the dry weight proportions, and the mean weight diameter (MWD), geometric mean diameter (GMD) and aggregate disintegration rate (PAD) were calculated from the mass proportions. The contents of various active organic carbon fractions within aggregates of different particle sizes were also determined.

2.2.7. Mineralization and Turnover Characteristics of Soil Organic Carbon

The mineralization and turnover characteristics of soil organic carbon were determined using the method of [32] by indoor constant temperature aerobic cultivation at 25 °C. The soil moisture content was adjusted to 60% of the field water holding capacity and then sealed in the dark for cultivation. The alkaline solution captured and released CO_2, and the cumulative mineralized carbon content was measured by periodic titration. A dual reservoir first-order kinetic model was used to fit the data, and parameters such as potential mineralized organic carbon pool, organic carbon mineralization rate constant, organic carbon half turnover period, carbon mineralization entropy, activated carbon pool turnover time, and stable carbon pool turnover time were calculated to characterize the turnover law of soil carbon mineralization.

2.2.8. Soil Total Nitrogen and Nitrogen Storage

The soil total nitrogen content was determined by the Kjeldahl digestion method with a concentrated sulfuric acid mixed catalyst, and the nitrogen concentration of the digestion solution was analyzed with a continuous flow analyzer. Soil bulk density was determined for the 0–20 cm and 20–40 cm layers, and nitrogen storage ($kg\ m^{-2}$) was calculated layer by layer from soil thickness and total nitrogen content and summed to obtain the total nitrogen storage of the 0–40 cm soil profile.

2.2.9. Inorganic Nitrogen Components in Soil

Soil nitrate nitrogen and ammonium nitrogen were extracted by constant temperature oscillation of 2 $mol{\cdot}L^{-1}$ potassium chloride solution, and the filtrate was measured for content by an AA continuous flow analyzer; soil alkaline nitrogen is absorbed at a constant temperature using the alkaline diffusion method, and its content is calculated by standard acid titration.

2.2.10. Acid Hydrolyzed Organic Nitrogen Components

Referring to the method proposed in [33], a high-temperature reflux acid hydrolysis method using 6 mol L^{-1} hydrochloric acid was used to determine the acid hydrolysis of soil samples. The soil samples were sieved through a 0.15 mm sieve and placed in a hydrolysis tube. After sealing with sufficient hydrochloric acid solution, they were subjected to constant temperature condensation reflux at 110 °C for 6 h to complete the acid hydrolysis treatment. After the hydrolysis was completed and cooled, all the acid hydrolysis filtrate was filtered

and collected to volume. The total acid hydrolysis nitrogen content in the filtrate was determined using an AA continuous flow analyzer, and then the amino acid nitrogen and amino sugar nitrogen content were quantitatively detected by characteristic color reaction combined with the instrument. The unknown acid hydrolysis nitrogen content was obtained by subtracting the amino acid nitrogen and amino sugar nitrogen content from the total acid hydrolysis nitrogen value. The soil total nitrogen was simultaneously measured. Subtract the total acid hydrolyzable nitrogen content from the total nitrogen content to obtain the non-acid hydrolyzable nitrogen content.

2.3. Statistical Analysis

The structural equation model (SEM) used R-package lavaan. Model fitness was evaluated using χ^2, χ^2/df, GFI, and RMSEA; acceptable model fit was defined as $\chi^2/df < 3$, GFI > 0.90, RMSEA < 0.08. Both direct and indirect standardized effects were calculated to disentangle causal pathways. Variance inflation factor (VIF) was calculated to detect multicollinearity among predictor variables prior to model construction. Path coefficients exceeding 1.0 were carefully checked against VIF outputs. All analyses were conducted using R (4.1.2). Data and graphs were processed using Microsoft Office Excel 2017 (Microsoft Windows, Redmond, WA, America) and analysis of variance (ANOVA) was performed using SPSS software (IBM Statistics 21.0, New York, NY, America). Differences between the treatments were analyzed using the least significant difference (LSD) test at the 0.05 probability level.

3. Results and Analysis

3.1. Maize Yield

Maize yield was determined at the mature stage after the 13th consecutive growing season (Figure 1). Compared with M0, organic substitution treatments (M25, M50, M100) increased maize yield. M50 obtained the highest maize yield among all treatments. N0 showed the lowest maize yield, which was significantly lower than M50. M25 and M100 had intermediate yield levels without significant differences with M0. Compared with M0, the yield of M25, M50 and M100 increased by 7.95%, 14.80% and 9.40%, respectively. Among all organic substitution treatments, M50 achieved the optimal yield-increasing effect. The average maize yield of M50 was 6.41% higher than the average levels of M25 and M100.

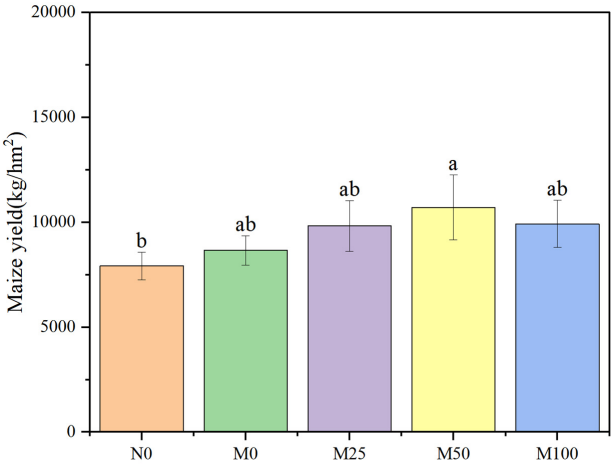


Figure 1. Effects of different organic–inorganic substitution ratios on maize yield. Bars represent mean ± SE (n = 3). Different lowercase letters indicate significant differences among treatments at $p < 0.05$.

3.2. Organic Carbon Content and Organic Carbon Reserve

Compared with M0, organic substitution treatments in various soil layers significantly increased soil organic carbon content and soil organic carbon storage (Figure 2). The improvement range in the 0–20 cm soil layer was 28.95~34.21%, and the 20–40 cm soil layer was 14.81~40.74%. The improvement range of soil organic carbon storage in the 0–20 cm soil layer reached 24.32~37.84%, and the 20–40 cm soil layer was 20.00~28.00%. Among all organic substitution treatments, M100 had the best carbon sequestration effect. The average soil organic carbon content in the two layers increased by 11.45% compared with the average levels of M25 and M50, and the average soil organic carbon storage in the two layers increased by 6.82% compared with the other two groups of organic substitution treatments. The initial SOM content of 19.4 g kg^{-1} in 2012 indicated the depleted carbon pool of the degraded black soil; the significant increases in SOC content and storage under organic substitution relative to M0 substantiate the effective restoration of the soil carbon pool.

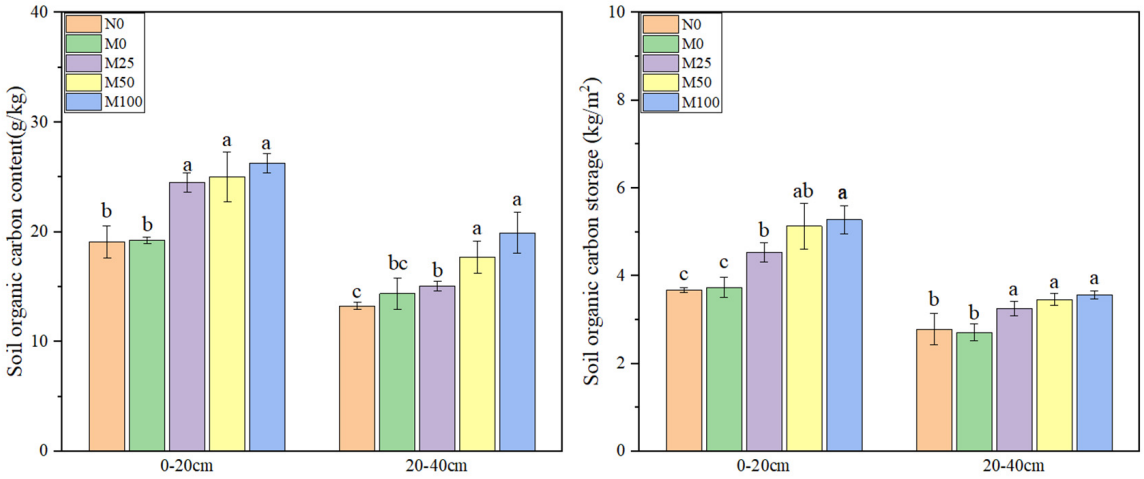


Figure 2. Effects of different organic-to-inorganic substitution ratios on organic carbon content and organic carbon reserves in black soil. Bars represent mean ± SE (n = 3). Different lowercase letters indicate significant differences among treatments at $p < 0.05$.

3.3. Classification of Soil Organic Carbon Components

3.3.1. Active Organic Carbon Components

Compared with M0, the organic substitution treatment in each soil layer improved easily oxidizable carbon content, microbial biomass carbon content, soluble organic carbon and particle organic carbon content (Table 3). The increase in the easily oxidizable carbon content in the 0–20 cm and 20–40 cm soil layers was 8.62~31.74% and 32.87~53.80%, the increase in the microbial biomass carbon content in the 0–20 cm and 20–40 cm soil layers was 20.49~66.58% and 40.03~79.11%, the increase in soluble organic carbon in the 0–20 cm and 20–40 cm soil layers was 25.00~50.56% and 0.33~41.91%, and the increase in particle organic carbon content in the 0–20 cm and 20–40 cm soil layers was 26.67~40.00% and 23.81~52.38%. Among all the organic substitution treatments, M50 showed the best effect in improving soil active organic carbon fractions, with easily oxidizable carbon content, microbial biomass carbon content, soluble organic carbon and particle organic carbon content increasing by 12.41%, 19.08%, 14.22%, and 10.14%, compared with M25 and M100.

Table 3. Effects of different organic-to-inorganic ratios on active organic carbon content in black soil. Different lowercase letters indicate significant differences among treatments at $p < 0.05$.

Soil Layer	Treatment	Easily Oxidizable Carbon Content (mg/kg)	Microbial Biomass Carbon Content (mg/kg)	Soluble Organic Carbon (mg/kg)	Particle Organic Carbon Content (g/kg)
0–20 cm	N0	415 ± 51.9 d	190.9 ± 12.9 c	35.7 ± 3.8 c	2.8 ± 0.2 d
	M0	497.4 ± 17 c	198.1 ± 16.9 c	35.6 ± 1.7 c	3.0 ± 0.2 cd
	M25	550.3 ± 61.1 bc	238.7 ± 8.5 b	44.5 ± 4.1 b	3.8 ± 0.1 ab
	M50	655.3 ± 34 a	329.1 ± 30.4 a	53.6 ± 6.1 a	4.2 ± 0.5 a
	M100	540.2 ± 18.5 b	321.4 ± 27.9 a	51.6 ± 6.5 ab	3.8 ± 0.4 ab
20–40 cm	N0	319.5 ± 16.1 c	137.4 ± 12.2 c	23.2 ± 2.2 c	2.0 ± 0.2 c
	M0	299 ± 29.4 c	126.4 ± 2.8 c	30.3 ± 0.6 b	2.1 ± 0.2 c
	M25	397.8 ± 54.7 b	176.6 ± 20.7 b	30.4 ± 2.9 b	2.6 ± 0.2 b
	M50	460.5 ± 18.1 a	226.6 ± 27.6 a	43.0 ± 3.6 a	3.2 ± 0.3 a
	M100	409.3 ± 30.3 b	214.2 ± 27 a	33.5 ± 2.4 b	2.9 ± 0.5 ab

3.3.2. Stable Organic Carbon Components

Compared with M0, organic substitution treatments in each soil layer increased heavy fraction organic carbon, mineral-bound organic carbon and stubborn organic carbon content (Figure 3). The increase in heavy fraction organic carbon in the 0–20 cm and 20–40 cm soil layers ranged from 0.00% to 18.89% and 22.73% to 41.82%, respectively; the increase in mineral-bound organic carbon in the 0–20 cm and 20–40 cm soil layers ranged from 6.67% to 33.33% and 4.55% to 18.18%, respectively; and the increase in stubborn organic carbon in the 0–20 cm and 20–40 cm soil layers ranged from 5.71% to 21.43% and 5.00% to 20.00%, respectively. Among all organic substitution treatments, M100 exhibited the optimal effect in accumulating soil stable organic carbon fractions. Compared with the average levels of M25 and M50, its heavy fraction organic carbon, mineral-bound organic carbon and stubborn organic carbon content increased by 12.17%, 12.28%, and 6.75%, respectively.

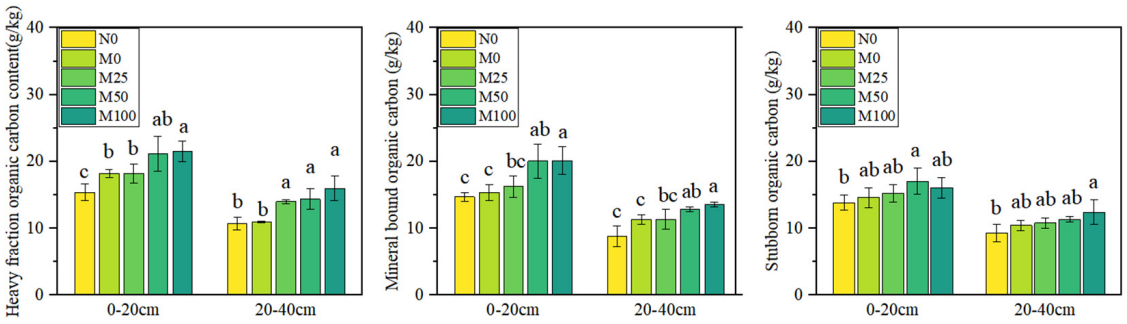


Figure 3. The effect of different organic-to-inorganic ratios on the stability and organic carbon content in black soil. Bars represent mean ± SE (n = 3). Different lowercase letters indicate significant differences among treatments at $p < 0.05$.

3.3.3. Humus Carbon Components

Compared with M0, organic substitution treatments in each soil layer increased humic acid carbon, humin carbon and fulvic acid carbon (Figure 4). The increased ranges of humic acid carbon in the 0–20 cm and 20–40 cm soil layers were 11.63~34.88% and 17.86~21.43%, the increased ranges of humin carbon in each soil layer were 7.41~8.89% and 6.10~26.83%, and the increased ranges of fulvic acid carbon in each soil layer were 11.11~44.44% and 11.76~41.18%. Among all organic substitution treatments, M100 showed the best effect in promoting the accumulation of three humus carbon fractions, with humic acid carbon,

humin carbon and fulvic acid carbon increasing by 9.64%, 6.53% and 14.07% compared with the average level of M25 and M50.

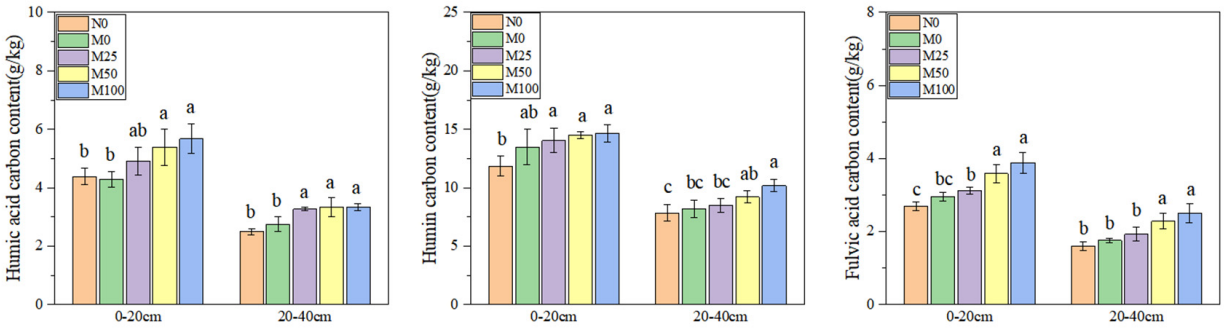


Figure 4. The effect of different ratios of organic and inorganic matter on the content of humic acid carbon components in black soil. Bars represent mean ± SE (n = 3). Different lowercase letters indicate significant differences among treatments at $p < 0.05$.

3.4. Soil Water-Stable Aggregates and Bound Carbon

3.4.1. Aggregate Particle Size Distribution

Compared with M0, the organic substitution treatment in each soil layer increased the proportion of large aggregates >2 mm and 0.25–2 mm while reducing the proportion of microaggregates by 0.053–0.25 mm and <0.053 mm (Figure 5). The increase in >2 mm aggregates in the 0–20 cm soil layer was 80.00~225.00%, the increase in 0.25–2 mm aggregates was 25.13~47.21%, the decrease in 0.053–0.25 mm aggregates was 6.00~14.00%, and the decrease in <0.053 mm aggregates was 8.11~18.92%. The increase in soil aggregates >2 mm in the 20–40 cm soil layer was 45.33~116.67%, the increase in aggregates of 0.25–2 mm was 11.11~55.56%, the decrease in aggregates of 0.053–0.25 mm was 4.10~16.23%, and the decrease in aggregates <0.053 mm was 2.94~8.82%. Among all the organic substitution treatments, M100 had the best effect on optimizing the particle size composition of soil aggregates. The average values of large aggregates >2 mm and 0.25–2 mm in the two layers were 18.52% and 12.05% higher than the average levels of M25 and M50, respectively. The average values of microaggregates of 0.053–0.25 mm and <0.053 mm in the two layers were 5.84% and 4.79% lower than the average values of the other two organic substitution treatments, respectively.

3.4.2. Stability Parameters of Aggregates

Compared with M0, organic substitution treatments in each soil layer increased the average weight diameter (MWD) and geometric mean diameter (GMD) and reduced the aggregate disintegration rate (Table 4). The average weight diameter from 0–20 cm increased by 24.62% to 56.92%, and from 20–40 cm by 30.59% to 63.53%. The geometric mean diameter from 0–20 cm increased by 11.11% to 50.00%, and from 20–40 cm by 3.23% to 32.26%. The aggregate disintegration rate from 0–20 cm decreased by 29.67% to 54.24%, and from 20–40 cm by 18.01% to 49.44%. Among all organic substitution treatments, M100 exhibited relatively higher aggregate stability-related indicators (MWD, GMD) and a lower aggregate disintegration rate; its two-layer average MWD and GMD increased by 14.17% and 12.79% compared with the average of M25 and M50, respectively, and the two-layer average aggregate disintegration rate decreased by 21.82% compared with the average of the other two organic substitution treatments.

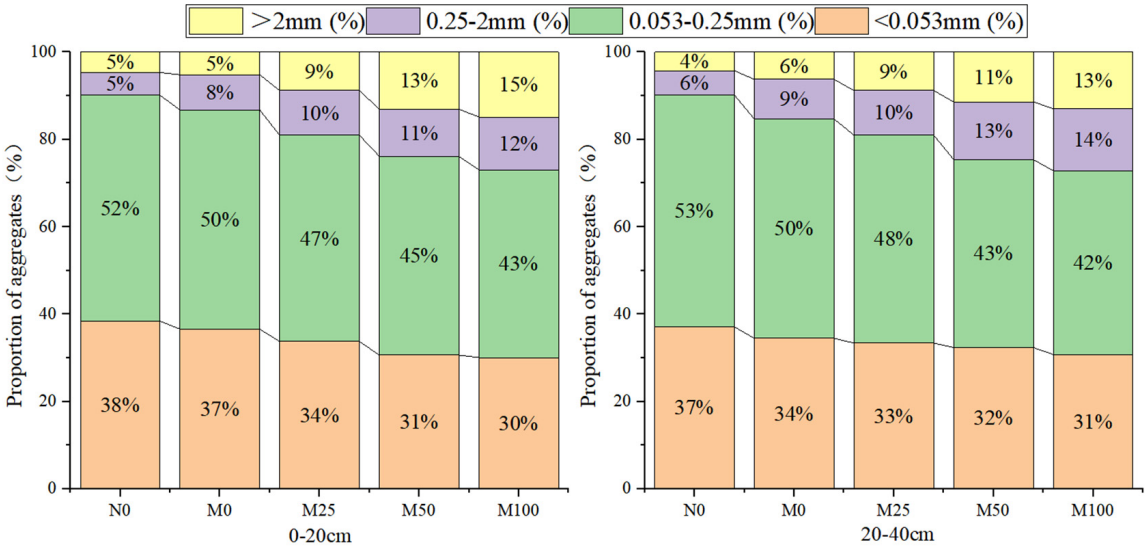


Figure 5. Effects of different organic-to-inorganic ratios on particle size distribution of black soil aggregates.

Table 4. Effects of different organic-to-inorganic ratios on stability parameters of black soil aggregates. Different lowercase letters indicate significant differences among treatments at $p < 0.05$.

Treatment	Average Weight-Diameter Ratio (MWD) (mm)		Geometric Mean Diameter (GMD) (mm)		Aggregate Disintegration Rate (%)	
	0–20 cm	20–40 cm	0–20 cm	20–40 cm	0–20 cm	20–40 cm
N0	1.33 ± 0.11 a	0.88 ± 0.08 a	0.80 ± 0.04 a	0.53 ± 0.03 a	35.50 ± 3.28 d	41.86 ± 5.34 e
M0	1.30 ± 0.11 a	0.85 ± 0.04 a	0.90 ± 0.04 b	0.62 ± 0.06 b	38.16 ± 0.88 e	39.08 ± 4.35 d
M25	1.62 ± 0.20 b	1.10 ± 0.16 b	1.00 ± 0.04 c	0.64 ± 0.03 b	26.84 ± 2.50 c	32.04 ± 2.65 c
M50	1.90 ± 0.27 c	1.20 ± 0.05 c	1.23 ± 0.11 d	0.73 ± 0.07 c	21.03 ± 1.33 b	25.32 ± 1.39 b
M100	2.04 ± 0.23 d	1.39 ± 0.18 d	1.35 ± 0.12 e	0.82 ± 0.06 d	17.46 ± 2.45 a	19.76 ± 1.76 a

3.4.3. Content of Activated Carbon in Various Forms of Aggregates

Compared with M0, organic substitution treatments in various soil layers increased the content of organic carbon, easily oxidizable organic carbon, microbial biomass carbon, soluble organic carbon, and particulate organic carbon at different particle sizes (Figure 6). The increase in organic carbon at 0–20 cm was 10.53~38.89%, 12.50~42.86% at 20–40 cm; the increase in easily oxidizable organic carbon at 0–20 cm was 14.29~42.86%, 16.67~45.83% at 20–40 cm; the increase in microbial biomass carbon at 0–20 cm was 12.00~48.00%, 14.81~51.85% at 20–40 cm; the increase in soluble organic carbon at 0–20 cm was 15.38~53.85%, 18.18~59.09% at 20–40 cm; and the increase in particulate organic carbon at 0–20 cm reached 11.76% to 41.18%, while from 20–40 cm it was 13.33% to 46.67%. Among all organic substitution treatments, M100 exhibited the optimal effect in promoting the accumulation of active organic carbon components at different particle sizes. The average levels of organic carbon, easily oxidizable organic carbon, microbial biomass carbon, soluble organic carbon, and particulate organic carbon at different particle sizes increased by 10.12%, 12.37%, 14.21%, 15.46%, and 9.87% compared with the average levels of M25 and M50.

3.5. Mineralization and Turnover Characteristics of Soil Organic Carbon

Compared with M0, organic substitution treatments in all soil layers increased the cumulative organic carbon mineralization and daily average organic carbon mineralization rate (Figure 7). The cumulative organic carbon mineralization increased by 21.32~45.71% at

0–20 cm and 18.92~43.24% at 20–40 cm. The daily average organic carbon mineralization rate increased by 14.29~37.14% at 0–20 cm and 11.32~32.08% at 20–40 cm. Among all organic substitution treatments, M100 exhibited the strongest promotion effect on soil organic carbon mineralization; its cumulative organic carbon mineralization and daily average organic carbon mineralization rate increased by 11.86% and 13.47%, respectively, compared with the average levels of M25 and M50.

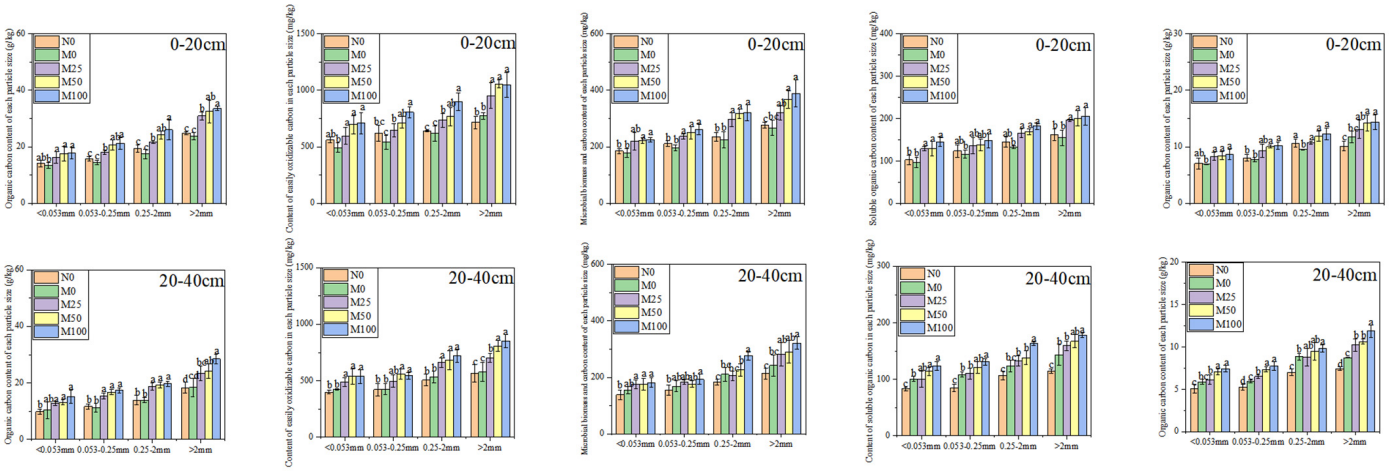


Figure 6. Effects of different organic-to-inorganic ratios on the content of various forms of activated carbon in black soil aggregates. Bars represent mean ± SE (n = 3). Different lowercase letters indicate significant differences among treatments at $p < 0.05$.

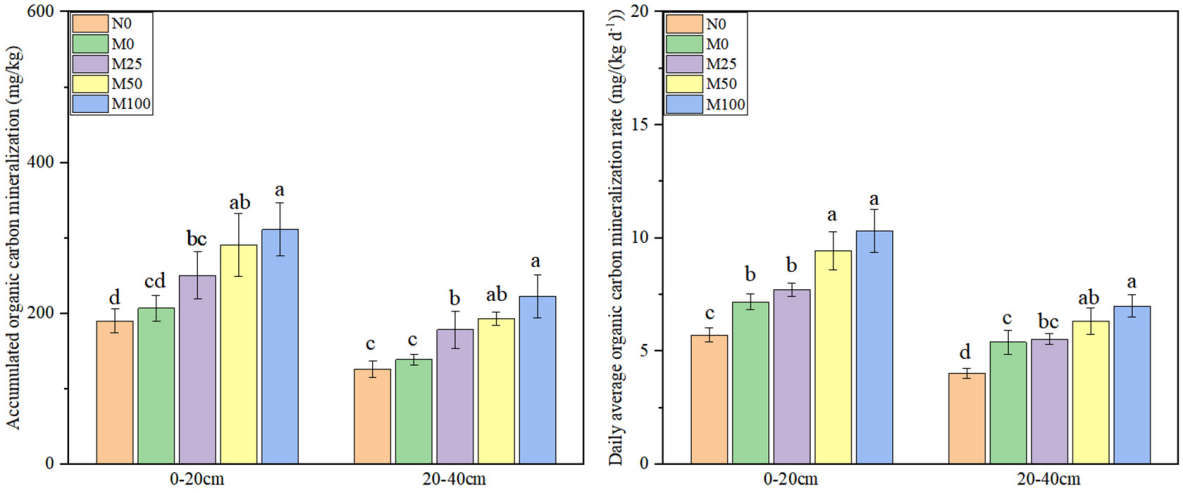


Figure 7. Effects of different organic-to-inorganic ratios on the mineralization and turnover characteristics of organic carbon in black soil. Bars represent mean ± SE (n = 3). Different lowercase letters indicate significant differences among treatments at $p < 0.05$.

Compared with M0, organic substitution treatments in each soil layer increased the potential mineralized organic carbon pool and organic carbon mineralization entropy, shortened the organic carbon half-life and the turnover time of the activated carbon pool; the turnover time of the stable carbon pool decreased with the rising organic substitution ratio (Table 5). The potential mineralized organic carbon pool increased by 12.97~27.14% at 0–20 cm and by 16.55~45.09% at 20–40 cm. The organic carbon mineralization entropy increased by 0.81~19.51% at 0–20 cm and decreased slightly or increased by up to 1.68% at 20–40 cm. The organic carbon half-life decreased by 0.04~6.13% at 0–20 cm and by 2.37~9.65% at 20–40 cm. The activated carbon pool turnover time decreased by 11.32~13.82%

at 0–20 cm and by 0.31~14.07% at 20–40 cm. The stable carbon pool turnover time decreased by 2.03~4.97% at 0–20 cm and by 7.41~19.50% at 20–40 cm. Among all organic substitution treatments, M100 achieved the optimal regulation of soil organic carbon turnover characteristics. Compared with the average levels of M25 and M50, its two-layer average potential mineralized organic carbon pool and organic carbon mineralization entropy increased by 12.14% and 8.93%, respectively; meanwhile, the two-layer average organic carbon half-life, activated carbon pool turnover time and stable carbon pool turnover time were shortened by 3.96%, 7.28% and 6.17%, respectively.

Table 5. Effects of different organic-to-inorganic substitution ratios on organic carbon mineralization in black soil. Different lowercase letters indicate significant differences among treatments at $p < 0.05$.

Treatment		Potential Mineralized Organic Carbon Pool ($mgkg^{-1}$)	Organic Carbon Mineralization Rate Constant (d^{-1})	Organic Carbon Half-Life (d)	Carbon Mineralization Entropy (%)	Activated Carbon Pool Turnover Time (d)	Stable Carbon Pool Turnover Time (Years)
0–20 cm	N0	196.21 ± 18 d	0.03 ± 0 a	24.72 ± 2 a	1.21 ± 0 d	18.67 ± 2 a	123.94 ± 10 ab
	M0	286.18 ± 7 bc	0.03 ± 0 a	23.14 ± 1 ab	1.23 ± 0 cd	18.38 ± 1 a	110.97 ± 4 b
	M25	282.80 ± 26 bc	0.03 ± 0 a	21.99 ± 3 bc	1.24 ± 0 c	16.20 ± 1 bc	123.75 ± 15 ab
	M50	320.17 ± 20 b	0.03 ± 0 a	23.37 ± 3 ab	1.33 ± 0 b	15.30 ± 2 c	125.38 ± 4 a
	M100	363.84 ± 51 a	0.03 ± 0 a	21.71 ± 3 c	1.47 ± 0 a	16.27 ± 1 bc	114.34 ± 12 b
20–40 cm	N0	137.10 ± 17 d	0.02 ± 0 b	27.39 ± 3 a	1.10 ± 0 c	21.82 ± 0 a	136.49 ± 16 ab
	M0	178.80 ± 20 c	0.03 ± 0 a	27.44 ± 3 a	1.19 ± 0 a	19.54 ± 2 b	142.80 ± 5 a
	M25	208.51 ± 17 bc	0.02 ± 0 b	26.70 ± 1 ab	1.11 ± 0 c	19.93 ± 1 b	129.93 ± 2 bc
	M50	240.37 ± 13 ab	0.03 ± 0 a	24.09 ± 3 bc	1.11 ± 0 c	19.88 ± 1 b	122.20 ± 11 cd
	M100	258.63 ± 23 a	0.03 ± 0 a	24.79 ± 2 c	1.17 ± 0 b	16.79 ± 1 c	114.97 ± 12 d

3.6. Soil Nitrogen Forms and Components

3.6.1. Total Nitrogen and Nitrogen Storage

Compared with M0, organic substitution treatments in all soil layers increased soil total nitrogen content and total nitrogen storage (Figure 8). The increase in soil total nitrogen content at 0–20 cm was 19.05~47.62% and at 20–40 cm was 15.38~53.85%. The increase in soil total nitrogen storage at 0–20 cm was 14.29~32.65% and at 20–40 cm was 18.52~40.74%. Among all organic substitution treatments, M100 exhibited the optimal effect on promoting soil nitrogen accumulation. Compared with the average levels of M25 and M50, its two-layer average total nitrogen content increased by 19.36%, and its two-layer average total nitrogen storage increased by 18.94%. Given the initial (2012) topsoil total nitrogen content of 1.033 g kg^{-1}, the elevated total nitrogen content and storage under organic substitution relative to M0 demonstrated the restoration of the soil nitrogen pools in the degraded black soil.

3.6.2. Inorganic Nitrogen Forms

Compared with M0, organic substitution treatments increased the proportion of ammonium nitrogen, while the proportion of alkali-hydrolyzed nitrogen decreased (Figure 9). The proportion of nitrate nitrogen showed an overall trend of first increasing and then decreasing with the rise in the organic substitution ratio. The proportion of ammonium nitrogen increased by 76.92~169.23% at 0–20 cm and 59.12~109.25% at 20–40 cm, while the proportion of alkali-hydrolyzed nitrogen decreased by 10.17~15.25% at 0–20 cm and 1.54~4.62% at 20–40 cm. The proportion of nitrate nitrogen fluctuated by −46.43%~−28.57% at 0–20 cm and continued to decrease by 23.17~50.32% at 20–40 cm. Among all organic substitution treatments, M100 exhibited the optimal effect on optimizing the distribution of soil inorganic nitrogen components. Compared with the average levels of M25 and M50,

its two-layer average proportion of ammonium nitrogen increased by 11.74%, whereas the two-layer average proportions of alkali-hydrolyzed nitrogen and nitrate nitrogen decreased by 3.68% and 17.26%, respectively.

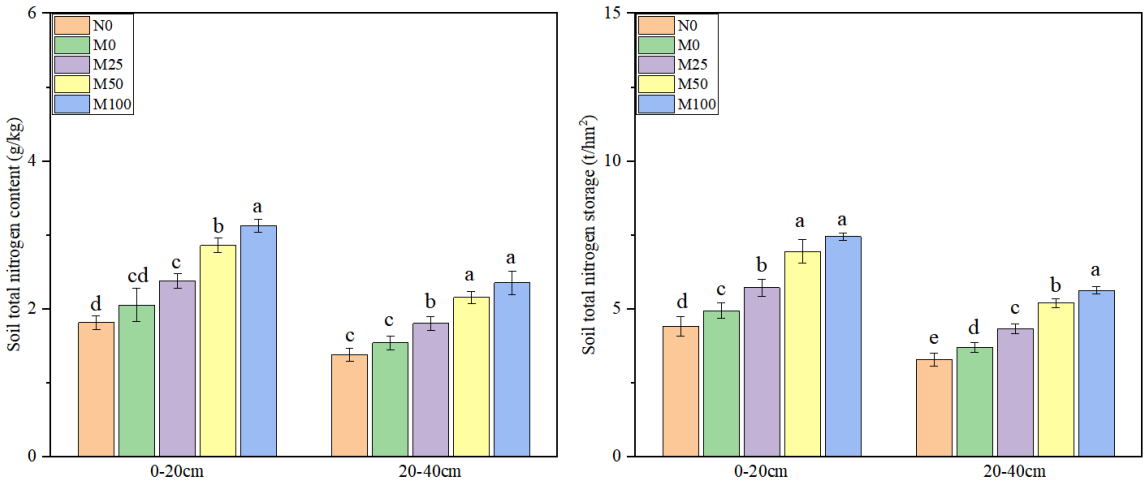


Figure 8. Effects of different organic-to-inorganic ratios on total nitrogen and nitrogen storage in black soil. Bars represent mean ± SE (n = 3). Different lowercase letters indicate significant differences among treatments at $p < 0.05$.

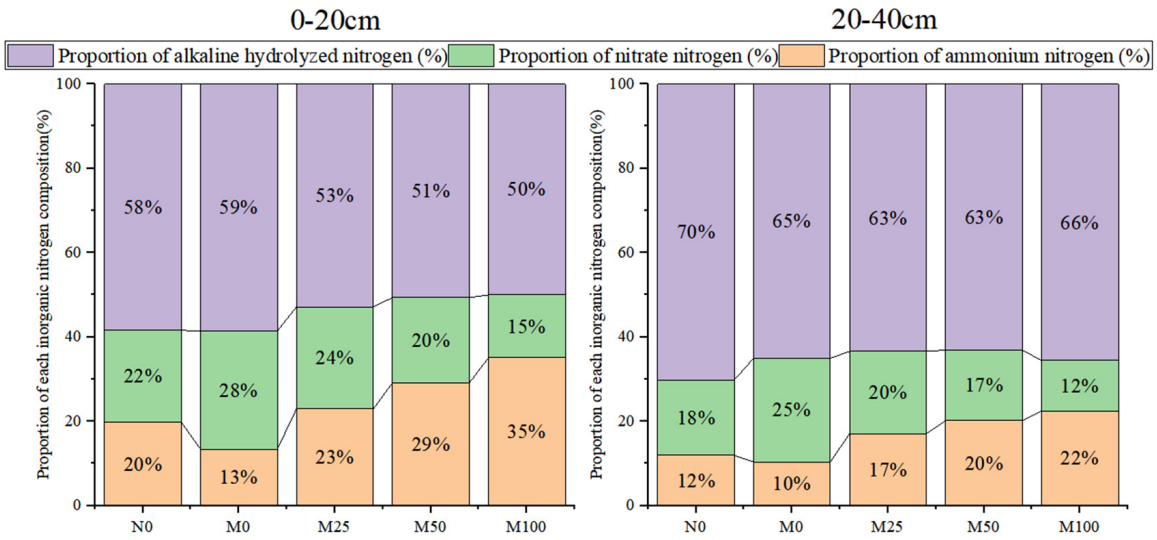


Figure 9. Effects of different organic-to-inorganic substitution ratios on contents of inorganic nitrogen fractions in black soil.

3.6.3. Acid-Hydrolyzed Organic Nitrogen Components

Compared with M0, organic substitution treatments modified the proportions of soil acid-hydrolyzable organic nitrogen fractions in both soil layers (Figure 10). In the 0–20 cm soil layer, amino acid nitrogen increased by 5.00–15.00%. Amino sugar nitrogen remained unchanged under M25 but rose by 20.00% under M50 and M100. Acid-hydrolyzable total nitrogen decreased by 2.38% under M25 and increased by 4.76–7.14% under M50 and M100. Unknown nitrogen slightly decreased by 5.26% under M25 and M50 and returned to the M0 level under M100. The proportion of non-acid-hydrolyzable nitrogen decreased by 13.23–33.13%. In the 20–40 cm soil layer, amino acid nitrogen decreased by 5.56% under M25, stayed consistent with M0 under M50, and increased by 22.05% under M100. Amino sugar nitrogen increased by 25.00% across all substitution treatments. Acid-hydrolyzable

total nitrogen was unchanged under M25 and increased by 7.14% under M50 and 4.76% under M100. Unknown nitrogen increased by 11.34% under M25 and remained identical to M0 under M50 and M100. Non-acid-hydrolyzable nitrogen decreased by 11.11–33.33%. Among all organic substitution treatments, M100 exhibited the optimal regulation on the distribution of soil acid-hydrolyzable organic nitrogen fractions. Relative to the average values of M25 and M50, the two-layer average proportions of amino acid nitrogen, amino sugar nitrogen, acid-hydrolyzable total nitrogen and unknown nitrogen in M100 increased by 3.47%, 8.26%, 1.10% and 2.45%, respectively, while the two-layer average proportion of non-acid-hydrolyzable nitrogen decreased by 12.96%.

3.7. Structural Equation Model

The structural equation model (SEM) used the R-package lavaan (Figure 11). Before model construction, variance inflation factor (VIF) analysis was implemented to detect multicollinearity among predictor variables; variables exhibiting severe collinearity (VIF > 5) were excluded from the model. Model fitness was evaluated using χ^2, χ^2/df, GFI, and RMSEA; acceptable model fit was defined as, GFI > 0.90, RMSEA < 0.08. Standardized direct, indirect and total effects were calculated to disentangle multi-step causal chains. The revised model exhibited acceptable fitting performance with $\chi 2 = 42.17$, $\chi^2/df = 2.41$, GFI = 0.942, RMSEA = 0.068. Different organic substitution ratios had no significant direct effect on soil organic carbon (SOC) or maize yield but exerted prominent indirect positive total effects on SOC by modifying intermediate mediators. Specifically, higher substitution ratios first increased the proportion of >0.25 mm macroaggregates and humic acid carbon. Improved aggregate structure and humus carbon status further elevated easily oxidizable carbon content and SOC storage. Elevated SOC, in turn, produced a strong positive direct effect on maize yield (standardized path coefficient = 0.837, $p < 0.05$). Meanwhile, organic carbon storage negatively regulated activated carbon pool turnover time and carbon mineralization loss. Shorter turnover time and higher mineralization loss subsequently suppressed SOC accumulation, forming an internal counterbalancing loop within the soil system.

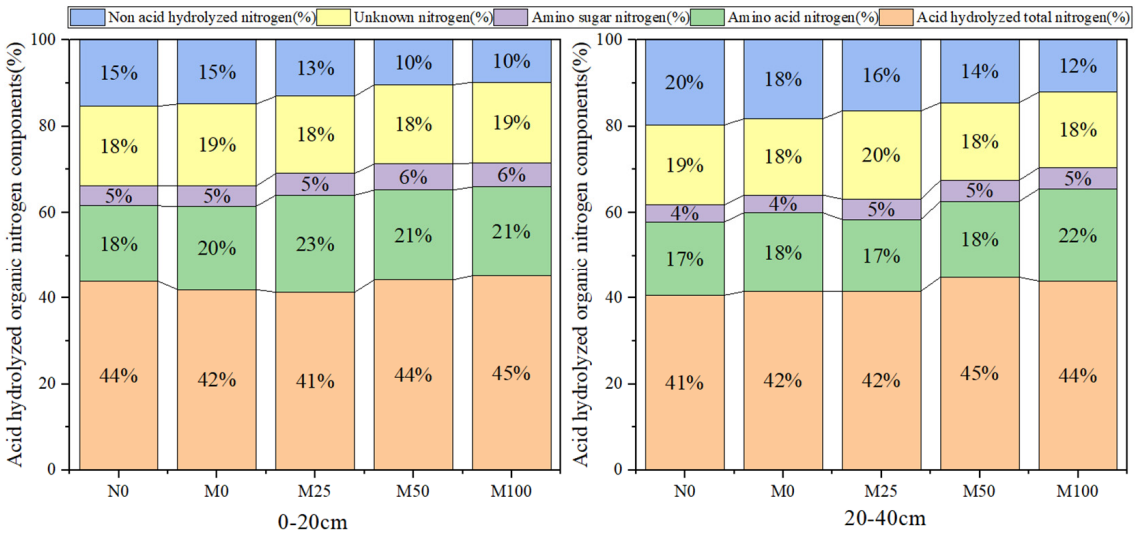


Figure 10. Effects of different ratios of organic matter to inorganic matter on contents of acid-hydrolyzable organic nitrogen fractions in black soil.

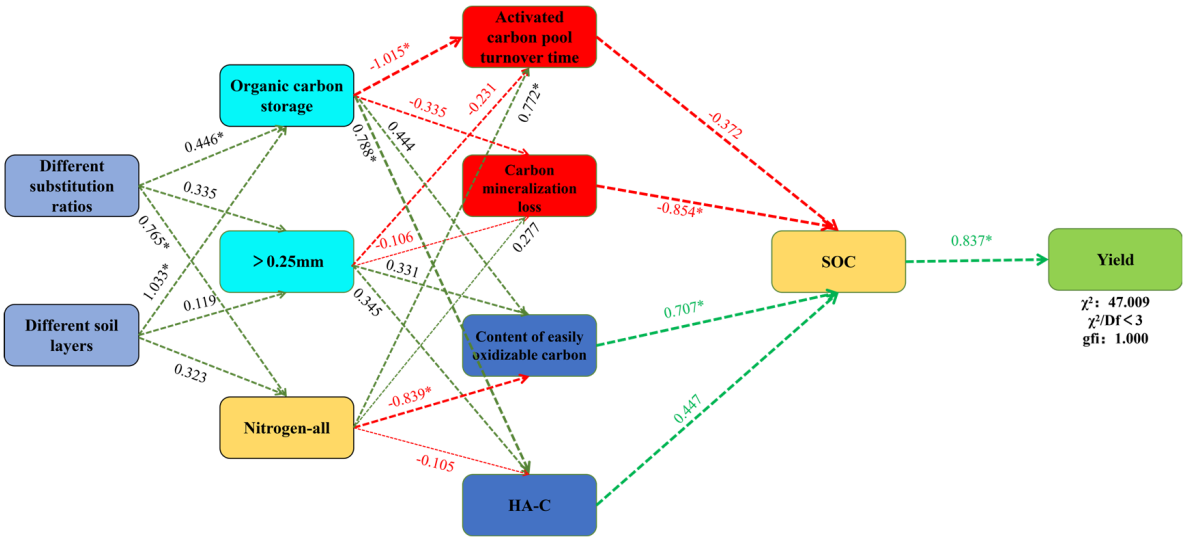


Figure 11. Structural equation model. Note: Green arrows in the figure indicate a positive correlation between variables, and red arrows indicate a negative correlation. "*" in the figure denotes statistical significance at $p < 0.05$.

4. Discussion

Soil carbon and nitrogen pools constitute the basis of black soil fertility, and their restoration under fertilization determines the effectiveness of degraded black soil management; however, how the equal nitrogen organic substitution ratio shapes carbon pool differentiation and its linkage with crop productivity remains unclear [5,34,35]. Long-term continuous application of sole chemical fertilizers and continuous maize monoculture have continuously disturbed the carbon–nitrogen balance of black soil, causing organic matter depletion, aggregate fragmentation and decreased nutrient storage capacity [4,36,37]. In this 13-year equal nitrogen field experiment, organic manure nitrogen substitution simultaneously restored the degraded black soil and sustained maize productivity. Compared with sole chemical fertilization (M0), organic substitution increased the maize yield by 7.95–14.80%, with M50 achieving the highest yield (+14.80%) and M100 maintaining a 9.40% increase without yield penalty. The yield gains were mainly driven by soil carbon accumulation: elevated SOC exerted a strong positive direct effect on maize yield (standardized path coefficient = 0.837, $p < 0.05$, SEM), demonstrating that restoration of the degraded black soil carbon pool was translated into crop productivity. Yield therefore serves as a central indicator of the effectiveness of organic substitution in restoring degraded black soil.

Soil water-stable aggregates are the core physical carriers of organic carbon storage and nutrient retention in black soil, and the long-term single application of chemical fertilizers without external organic binding material input is a key factor causing aggregate structure deterioration [38–40]. In this study, sole chemical fertilization (M0) did not increase the proportion of >0.25 mm macroaggregates in the 0–20 cm and 20–40 cm layers relative to the unfertilized control N0, and even slightly increased the aggregate disintegration rate, because single mineral nutrient input cannot supplement the polysaccharides, humus precursors and microbial extracellular secretions that bind aggregates. By contrast, organic substitution increased the proportion of >2 mm macroaggregates by 80.00–225.00% in the 0–20 cm layer and by 45.33–116.67% in the 20–40 cm layer, raised the mean weight diameter (MWD) by 24.62–63.53% and decreased the aggregate disintegration rate by 18.01–54.24% relative to M0, with M100 performing best. A spring base application of cattle manure inputs large amounts of fresh organic matter, which microorganisms transform into aromatic humus and polysaccharide binders that promote the formation of large macroaggregates;

meanwhile, soluble organic carbon migrates downward with precipitation, improving the aggregate properties of the 20–40 cm subsoil. The physical protection provided by the improved aggregate structure therefore forms the basis of the observed carbon and nitrogen accumulation.

Taken together, the coordinated observations across aggregate structure, labile stable carbon pool divergence and carbon mineralization provide integrated mechanistic insights for degraded Mollisols under equal nitrogen manure substitution. A distinct functional divergence was found between moderate and full substitution: M50 maximized the labile carbon fractions in the 0–20 cm topsoil, with easily oxidizable carbon and microbial biomass carbon 31.7% and 65.0% higher than M0, respectively, and the highest soluble organic carbon (655.3 mg kg^{-1}) and particulate organic carbon (4.2 g kg^{-1}), supporting rapid nutrient mineralization for maize short-term growth; in contrast, M100 accumulated more stable carbon fractions, with heavy fraction, mineral-bound and stubborn organic carbon 12.17%, 12.28% and 6.75% higher than the average of M25 and M50, respectively. Moderate organic carbon input provides sufficient easily decomposable substrates for microorganisms without excessive retention of fibrous organic matter, thereby rapidly increasing soil active carbon storage and continuously mineralizing available nutrients during the maize growth period [41–45]. Full organic substitution, although less effective in raising labile carbon in the short term, continuously inputs humified precursors that favor the accumulation of stable carbon components and long-term improvement of the aggregate structure [46–48]. Such divergence cannot be captured by single-indicator measurement, highlighting the necessity of evaluating both labile and stable carbon fractions together with aggregate properties when assessing fertilization-induced soil restoration.

Aerobic incubation and two-pool first-order kinetic fitting showed that, relative to M0, organic substitution increased the potential mineralizable carbon pool by 12.97–45.09%, raised the carbon mineralization entropy by 0.81–19.51% in the 0–20 cm layer, and shortened the organic carbon half-life by up to 9.65%, indicating accelerated carbon turnover. This finding differs from the traditional view that higher mineralized carbon indicates severe soil carbon loss. In our experiment, the physical protection of aggregates produced substantial carbon sequestration gains that offset mineralization-induced carbon loss: organic substitution increased 0–20 cm SOC storage by 24.32–37.84% and 20–40 cm SOC storage by 20.00–28.00% relative to M0. Under sole chemical fertilization, external carbon input is scarce and carbon cycling relies mainly on the decomposition of native soil organic matter, so carbon turnover and carbon sequestration show an antagonistic relationship; the simultaneous activation of labile carbon turnover and accumulation of stable carbon under organic fertilization achieves the coupling of carbon turnover and carbon sequestration [49,50], alleviating the organic carbon decline of black soil farmland in Northeast China from the root.

There is a close coupling relationship between soil carbon cycling and nitrogen transformation. Gradient organic fertilizer substitution drives the expansion of soil total nitrogen and the reconstruction of multi-level nitrogen components, addressing the shortcomings of single fertilizer applications such as low nitrogen use efficiency, high nitrogen loss risk and insufficient long-term nitrogen supply [51,52]. In this study, soil total nitrogen content and nitrogen storage in the 0–20 cm and 20–40 cm layers continued to increase with the rising substitution ratio and were highest under M100, because cattle manure brings large amounts of organically bound nitrogen that is physically encapsulated by aggregates and retained in the soil, reducing leaching and runoff losses [53]. In terms of inorganic nitrogen components, sole chemical fertilization (M0) produced a higher nitrate nitrogen proportion, the main source of nitrogen loss and farmland non-point source pollution, whereas organic substitution increased the ammonium nitrogen proportion by 59.12–169.23% and decreased

the nitrate nitrogen proportion by up to 50.32%. Organic matter input raises the soil C/N ratio, inhibits nitrifying bacteria, slows the conversion of ammonium to nitrate, and positively charged ammonium ions are readily adsorbed by black soil clay colloids, achieving long-term retention of available nitrogen and reducing nitrogen-leaching risk during the growth period [54]. In the acid-hydrolyzable organic nitrogen components, amino-acid nitrogen, amino-sugar nitrogen, acid-hydrolyzable total nitrogen and unknown nitrogen increased with the substitution ratio while the non-acid-hydrolyzable nitrogen proportion decreased, with M100 performing best; the organic fertilizer-stimulated proliferation of soil microorganisms continuously supplements slow-release nitrogen components such as amino-acid nitrogen and amino-sugar nitrogen, constructing a long-term slow-release nitrogen reservoir and balancing nitrogen supply throughout maize growth [55–59].

The stratification characteristics of soil profiles indicate that organic substitution improved the carbon, nitrogen and aggregate structure of the 0–20 cm topsoil more effectively than the 20–40 cm subsoil, while still effectively improving subsoil fertility, because the soluble carbon and nitrogen input from cattle manure migrates downward with water, continuously optimizing the subsoil structure and nutrient status [60]. The SEM verification showed that aggregate components, activated carbon pool turnover and carbon–nitrogen components were the key mediating factors through which organic substitution regulated soil carbon–nitrogen storage and crop yield: external organic carbon input increased the macroaggregate proportion and SOC storage, shortened the activated carbon pool turnover time, reduced carbon mineralization loss, and through multi-path positive synergy significantly enhanced maize yield. Because of the lack of external organic substrates, sole chemical fertilization cannot activate these regulatory pathways and can only guarantee short-term yield without achieving long-term improvement of black soil fertility. These profile scale observations stress that gradient organic substitution reshapes not only topsoil fertility but also subsoil carbon–nitrogen distribution, triggering functional differentiation among carbon pools rather than a simple linear increase of all carbon fractions; agronomic 'benefit' should therefore be differentiated by management goals, as short-term nutrient supply and long-term carbon sequestration cannot be maximized by a single substitution rate in degraded Mollisols. It should nevertheless be noted that the SEM was constructed with three field replicates and a single maize yield observation per treatment (n = 5 treatments); given the limited degrees of freedom for the yield path, the path coefficients should be interpreted with caution and the model regarded as exploratory.

The novelty of this study lies in its equal nitrogen gradient design, its integrated assessment of aggregate physical, carbon pool and nitrogen form responses on degraded Mollisols, and its identification of a substitution ratio-dependent functional trade-off between labile and stable carbon pools, extending beyond the general conclusions of long-term fertilizer experiments. Based on the 13-year equal nitrogen field experiment on degraded black soil in Gongzhuling, differentiated fertilization references are proposed for the study site. For pursuing short-term maize yield and higher labile nutrient pools under similar soil climatic conditions, 50% cattle manure N substitution may be considered; for long-term black soil restoration and farmland carbon sequestration, 100% manure N substitution showed promising performance in this experiment. Subsequent research can couple organic fertilizer gradient substitution with agronomic measures such as maize intercropping, no tillage and straw mulching to explore the synergistic effects of multiple measures on carbon sequestration and nutrient activation, and to establish regional graded organic fertilizer application standards matching different degrees of black soil degradation [61,62]. It should be noted that soil sampling was carried out only post-harvest of the 13th maize growing season; although soil carbon–nitrogen pools and aggregate properties reflect the cumulative effects of 13-year consecutive fertilization, crop yield and some soil indicators may still

be subject to inter-annual meteorological fluctuation. The fertilization recommendations should therefore be regarded as preliminary references under local soil–climate conditions, and multi-year continuous in situ monitoring combining long-term maize yield datasets is required to further verify the stability of substitution effects across years.

5. Conclusions

Under equal nitrogen input, long-term cattle manure nitrogen substitution effectively restored the carbon and nitrogen pools of degraded black soil under maize monoculture, as reflected in improved macroaggregate stability, elevated soil organic carbon and total nitrogen storage, and restructured carbon pool and nitrogen form composition. The substitution ratio determined the functional outcome: the 50% substitution maximized labile carbon fractions and maize yield, whereas the 100% substitution favored stable carbon accumulation and nitrogen retention without yield loss, indicating that there is no universal single optimal substitution rate and that fertilization strategies should match local management objectives. These results imply that organic nitrogen substitution couples soil carbon sequestration with nitrogen stabilization while sustaining crop productivity, providing a practical basis for chemical fertilizer reduction and black soil fertility restoration in Northeast China.

Author Contributions: L.W.: conceptualization, methodology, formal analysis, writing original draft. X.J.: investigation, laboratory analysis, data curation. D.L.: software, visualization. F.Z.: field experiment management, sample collection. B.W.: review and editing. H.W.: project administration, supervision, writing—review and editing. All authors have read and agreed to the published version of the manuscript.

Funding: This research was funded by the National Key Research and Development Program of China (grant number: 2024YFD1500300).

Data Availability Statement: All datasets generated and analyzed during the current study are included within the article.

Conflicts of Interest: The authors declare no conflicts of interest.

References

1. Wang, T.; Liu, L.; Huang, S. Study on the Influence of Policy Guidance and Market-Driven Factors on Farmers' Behavior Regarding Black Soil Protection. *Land* **2024**, *13*, 1082. [CrossRef]
2. Kong, D.; Chu, N.; Luo, C.; Liu, H. Analyzing Spatial Distribution and Influencing Factors of Soil Organic Matter in Cultivated Land of Northeast China: Implications for Black Soil Protection. *Land* **2024**, *13*, 1028. [CrossRef]
3. Zhang, F.; Han, P.; Wu, L.; Tian, Z. Quantitative Evaluation and Evolution Characteristics of Consistency Level of Black Soil Conservation Policy, Taking China's Black Soil Protection Policy as an Example. *Land* **2024**, *13*, 800. [CrossRef]
4. Jiang, M.; Jia, Z.; Wen, Y.; Xu, H.; Wang, H.; Zeng, Y.; Li, L.; Cui, M.; Li, H.; Zhang, J. Safeguarding the"Black Soil Granary": Innovations in Soil Conservation and Sustainable Agriculture. *Bull. Chin. Acad. Sci.* **2024**, *38*, 251–258. [CrossRef]
5. Wu, Z.; Uwiragiye, Y.; Han, X.; Feng, H.; Zhang, M.; Ji, Y.; Zhu, Y.; Chen, X.; Yan, J.; Lu, X.; et al. Long-term manure application enhances soil quality via aggregate-scale nutrient stock regulation in maize-soybean rotation. *Plant Soil* **2025**, *517*, 659–676. [CrossRef]
6. Liu, F.; Zhang, H.; Zeng, J.; Guo, Z. Assessment of Soil Degradation by Erosion in a Small Catchment in the Black Soil Region of Northeast China. *Soil Syst.* **2026**, *10*, 32. [CrossRef]
7. Yan, B.X.; Tang, J. Study on black soil erosion rate and the transformation of soil quality influenced by erosion. *Geogr. Res.* **2005**, *23*, 22–29. [CrossRef]
8. Jiang, F.; Peng, X.; Li, Q.; Qian, Y.; Zhang, Z. Potential Reduction of Spatiotemporal Patterns of Water and Wind Erosion with Conservation Tillage in Northeast China. *Land* **2024**, *13*, 1219. [CrossRef]
9. Novelli, L.E.; Caviglia, O.P.; Piñeiro, G. Increased cropping intensity improves crop residue inputs to the soil and aggregate-associated soil organic carbon stocks. *Soil Tillage Res.* **2017**, *165*, 128–136. [CrossRef]

10. Miao, X.; Li, Z.; Wang, M.; Mei, J.; Chen, J. Measurement of cultivated land ecosystem resilience in black soil region of Northeast China under the background of cultivated land protection policy in China: Case study of Qiqihar City. *J. Clean. Prod.* **2024**, *434*, 140141. [CrossRef]
11. Tang, H.; Qiu, J.; Ranst, E.V.; Li, C. Estimations of soil organic carbon storage in cropland of China based on DNDC model. *Geoderma* **2006**, *134*, 200–206. [CrossRef]
12. Ahmed, M.; Rau, M.; Mukhtar, Z.; Saeed, N.A. Excessive use of nitrogenous fertilizers: An unawareness causing serious threats to environment and human health. *Environ. Sci. Pollut. Res.* **2017**, *24*, 26983–26987. [CrossRef] [PubMed]
13. Li, A.; Shi, Z.; Yin, Y.; Fan, Y.; Zhang, Z.; Tian, X.; Yang, Y.; Pan, L. Excessive use of chemical fertilizers in catchment areas raises the seasonal pH in natural freshwater lakes of the subtropical monsoon climate region. *Ecol. Indic.* **2023**, *154*, 10. [CrossRef]
14. Sharratt, B.S.; Kennedy, A.C.; Hansen, J.C.; Schillinger, W.F. Soil Carbon Loss by Wind Erosion of Summer Fallow Fields in Washington's Dryland Wheat Region. *Soil Sci. Soc. Am. J.* **2018**, *82*, 1551–1558. [CrossRef]
15. Song, H.; Chang, Z.; Hu, X.; Li, Y.; Duan, C.; Yang, L.; Wang, H.; Li, T. Combined Application of Chemical and Organic Fertilizers Promoted Soil Carbon Sequestration and Bacterial Community Diversity in Dryland Wheat Fields. *Land* **2024**, *13*, 1296. [CrossRef]
16. Chang, Y.; Zhang, X.; Shu, Q.; Sun, Z.; Yang, M.; Liu, X.; Guo, J.; He, Z.; Li, L.; Huang, J.; et al. Effects of fertilization measures on soil fertility and crop yields in drylands of the North China Plain: A meta-analysis. *Front. Plant Sci.* **2026**, *17*, 1768991. [CrossRef] [PubMed]
17. Wang, X.; Chu, J.; Zhang, M.; Hou, M.; Zheng, K.; Lin, L.; Yan, Z.; Li, X.; Che, Z.; Song, H.; et al. Organic substitution for synthetic fertilizer mitigates the negative effects of warming on soil quality, greenhouse gas emissions, and soybean yields. *Field Crops Res.* **2026**, *336*, 110211. [CrossRef]
18. Zhang, F.; Wang, Y.; Wang, X.K.; Yan, C.; He, H.; Liu, S.; Zhang, G.; Han, J. Organic substitution improves crop productivity while mitigating the risk of soil reactive nitrogen losses: A meta-analysis of maize production in China. *J. Environ. Manag.* **2026**, *401*, 128774. [CrossRef] [PubMed]
19. Zhu, H.; Peng, Z.; Xu, X.; Qin, Y.; Yao, R.; Yang, J. Effect of Organic Substitution on the Improvement of Coastal Saline Farmland in Eastern China. *J. Soil Sci. Plant Nutr.* **2026**, *26*, 3021–3035. [CrossRef]
20. Wang, Q.; Wang, Y.; Li, Y.; Tian, X.; Li, X.; Wen, Y. Effects of the combination of biogas slurry and chemical fertilizer over three years on soil aggregate stability in Cambisols. *J. Soils Sediments* **2025**, *25*, 1201–1212. [CrossRef]
21. Crow, S.E.; Lajtha, K.; Filley, T.R.; Swanston, C.W.; Bowden, R.D.; Caldwell, B.A. Sources of plant-derived carbon and stability of organic matter in soil: Implications for global change. *Glob. Change Biol.* **2009**, *15*, 2003–2019. [CrossRef]
22. Xiang, X.; Chen, Y.; Lu, Y.; Chen, J.; Zhang, H.; Zhao, H.; Sun, S.; Zhai, S.; Tian, X. Biochar amendments enhanced organic carbon pool stability in soil aggregates by regulating soil carbon functional microbes. *Appl. Soil Ecol.* **2026**, *219*, 106811. [CrossRef]
23. Zhou, M.; Xiao, Y.; Xiao, L.; Li, Y.; Zhang, X.; Cruse, R.M.; Liu, X. Increased Soil Aggregate Stability by Altering Contents and Chemical Composition of Organic Carbon Fractions via Seven Years of Manure Addition in Mollisols. *Agriculture* **2023**, *13*, 88. [CrossRef]
24. Li, N.; You, M.-Y.; Zhang, B.; Han, X.-Z.; Panakoulia, S.; Yuan, Y.-R.; Liu, K.; Qiao, Y.-F.; Zou, W.-X.; Nikolaidis, N.; et al. Modeling Soil Aggregation at the Early Pedogenesis Stage from the Parent Material of a Mollisol Under Different Agricultural Practices. *Adv. Agron.* **2017**, *142*, 181–214. [CrossRef]
25. Yang, W.; Song, X.; He, Y.; Chen, B.; Zhou, Y.; Chen, J. Distribution of Soil Organic Carbon Density Fractions in Aggregates as Influenced by Salts and Microbial Community. *Land* **2023**, *12*, 2024. [CrossRef]
26. Zhang, Z.; Nie, J.; Liang, H.; Wei, C.-L.; Wang, Y.; Liao, Y.-L.; Lu, Y.-H.; Zhou, G.-P.; Gao, S.-J.; Cao, W.-D. The effects of co-utilizing green manure and rice straw on soil aggregates and soil carbon stability in a paddy soil in South China. *J. Integr. Agric.* **2022**, *22*, 1529–1545. [CrossRef]
27. Blair, G.J.; Lefroy, R.D.; Lisle, L. Soil carbon fractions based on their degree of oxidation, and the development of a carbon management index for agricultural systems. *Aust. J. Agric. Res.* **1995**, *46*, 1459–1466. [CrossRef]
28. Vance, E.D.; Brookes, P.C.; Jenkinson, D.S. An extraction method for measuring soil microbial biomass C. *Soil Biol. Biochem.* **1987**, *19*, 703–707. [CrossRef]
29. Xu, X.; Han, L.; Luo, X.; Liu, Z.; Han, S. Effects of nitrogen addition on dissolved N_2O and CO_2, dissolved organic matter, and inorganic nitrogen in soil solution under a temperate old-growth forest. *Geoderma* **2009**, *151*, 370–377. [CrossRef]
30. Wang, Q.; Shao, X.; Wu, Z.; Li, W. Effects of Different Organic Amendments on Aggregate-Associated Humus Carbons and Nutrients in a Paddy Soil. *Agronomy* **2025**, *15*, 2302. [CrossRef]
31. Plaza, C.; Giannetta, B.; Benavente, I.; Vischetti, C.; Zaccone, C. Density-based fractionation of soil organic matter: Effects of heavy liquid and heavy fraction washing. *Sci. Rep.* **2019**, *9*, 10146. [CrossRef] [PubMed]
32. Baldock, J.A.; Creamer, C.; Szarvas, S.; McGowan, J.; Carter, T.; Farrell, M. Linking decomposition rates of soil organic amendments to their chemical composition. *Soil Res.* **2021**, *59*, 630–643. [CrossRef]
33. Chantigny, M.H.; Olk, D.C.; Angers, D.A. Investigating the nature of soil carbohydrates and amino compounds with liquid chromatography. *Soil Sci. Soc. Am. J.* **2025**, *89*, e270018. [CrossRef]

34. Sharma, H.C.; Ren, W.; Lindsey, L.E.; Jacinthe, P.-A. Assessing the combined effect of tillage and nitrogen fertilizer rate on soil organic carbon sequestration using carbon isotope ratio. *Soil Tillage Res.* **2026**, *256*, 106845. [CrossRef]
35. Miao, J.; Liu, L.; Song, F.; Sun, H.; Ding, X.; Wang, J. Straw and nitrogen fertilization driving iron oxide transformation and soil carbon sequestration in saline paddy soils. *Front. Soil Sci.* **2026**, *6*, 1806071. [CrossRef]
36. Zhang, S.; Sun, L.; Jamshidi, A.H.; Niu, Y.; Fan, Z.; Zhang, H.; Liu, X.; Gao, L. Soil Degradation of Sloping Cropland in the Typical Black Soil Region in Northeast China: Risk Assessment and Uncertainty Analysis. *Land Degrad. Dev.* **2025**, *36*, 966–974. [CrossRef]
37. Sun, L.; Zhang, S.; Tang, W.; Jamshidi, A.H.; Xu, L.; Wang, Y.; Fan, Z.; Liu, X.; Gao, L. Mechanisms and key driving factors of erosion-induced degradation of sloping cropland in the typical black soil region in Northeast China. *Soil Tillage Res.* **2026**, *258*, 107037. [CrossRef]
38. Zhou, W.; Sun, X.; Li, S.; Du, T.; Zheng, Y.; Fan, Z. Effects of organic mulching on soil aggregate stability and aggregate binding agents in an urban forest in Beijing, China. *J. For. Res.* **2021**, *33*, 1083–1094. [CrossRef]
39. Song, W.; Liu, Z.; Li, X.; Min, X.; O'COnnor, D.; Li, J. Long-term recovery of aggregate-associated organic carbon in reclaimed mine soil. *Soil Tillage Res.* **2026**, *255*, 106791. [CrossRef]
40. Li, X.; Huang, R.; Xian, Y.M.; Tian, J.; Ma, X.; Yang, Q.; Li, B.; Wang, C. Characteristics of Organic Carbon Fractions and Carbon Dioxide Emissions of Different Size Aggregates in Rice Field Soils in Response to Long-Term Fertilization. *Sci. Agric. Sin.* **2026**, *59*, 1255–1271. [CrossRef]
41. Xue, Y.; Xia, F.; Ran, L.; Xu, Y.; Wu, H.; Wei, W.; Shi, Z.; Cai, X.; Wang, J. Maize Straw and Nitrogen Fertilizer Alter Soil Carbon and Nitrogen Mineralization during the Fallow Period in the Oasis Farmland area. *J. Soil Sci. Plant Nutr.* **2024**, *24*, 3663–3674. [CrossRef]
42. Zhang, L.; Liu, Z.K.; Jin, S.; Zhou, L.; Lin, Y.; Shi, S.; Shen, J.-P. Divergent response of surface and deep soil nitrogen mineralization to nitrogen and phosphorus additions in a subtropical forest. *Soil Ecol. Lett.* **2026**, *8*, 260420. [CrossRef]
43. Wang, C.; Lai, D.Y.F.; Wang, C.; Pan, T.; Zeng, C. Effects of rice straw incorporation on active soil organic carbon pools in a subtropical paddy field. *Soil Tillage Res.* **2015**, *152*, 8–16. [CrossRef]
44. Wang, Y.; Ao, D.; Wang, B.; Chen, Y.; Hu, Y.; Zhang, B.; Zhang, H.; Guo, W.; An, S. Particulate organic carbon dominates soil organic carbon dynamics in alpine ecosystems for its climate sensitivity and continuous storage. *CATENA* **2026**, *262*, 109607. [CrossRef]
45. Xu, M.G.; Yu, R.; Sun, X.F.; Liu, H.; Wang, B.R.; Li, J.M. Effects of long-term fertilization on labile organic matter and carbon management index(CMI) of the typical soils of China. *Plant Nutr. Fertil. Sci.* **2006**, *12*, 459–465. [CrossRef]
46. Chen, S.; Suo, Q.; Bao, W.; Liu, M.; Suo, Q. Cooling phase organic fertilizer applied in saline soil increase the content of soil macro-aggregates and aggregate-associated carbon. *PLoS ONE* **2025**, *20*, e0330756. [CrossRef] [PubMed]
47. Almendros, G.; González-Pérez, J.A. Soil Organic Carbon Sequestration Mechanisms and the Chemical Nature of Soil Organic Matter—A Review. *Sustainability* **2025**, *17*, 6689. [CrossRef]
48. Zhang, S.; Huang, F.; Guo, S.; Luo, Y.; Zhang, L.; Zhang, L.; Li, Z.; Ge, S.; Wang, H.; Fu, J. Mitigation of soil organic carbon mineralization in tea plantations through replacement of pruning litter additions with pruning litter derived biochar and organic fertilizer. *Ind. Crops Prod.* **2025**, *225*, 120518. [CrossRef]
49. Dou, X.; He, P.; Zhu, P.; Zhou, W. Soil organic carbon dynamics under long-term fertilization in a black soil of China: Evidence from stable C isotopes. *Sci. Rep.* **2016**, *6*, 21488. [CrossRef] [PubMed]
50. Meng, X.; Yu, H.; Zhang, X.; Li, Y.; Zamanian, K.; Yao, H. Fertilization Regimes and Nitrogen Cycling in Paddy Fields: Lessens for Agricultural Sustainability from a Meta-Analysis. *SSRN Electron. J.* **2022**. [CrossRef]
51. Parkinson, R.; Gibbs, P.; Burchett, S.; Misselbrook, T. Effect of turning regime and seasonal weather conditions on nitrogen and phosphorus losses during aerobic composting of cattle manure. *Bioresour. Technol.* **2004**, *91*, 171–178. [CrossRef] [PubMed]
52. Hou, H.; Ji, J.; Lan, X.; Drosos, M.; Liu, X.; Lv, Z.; Liu, Y.; Cheng, Z.; Zhou, W. Organic Fertilizers as Partial Substitutes for Chemical Fertilizers Enhance Nitrogen Immobilization and Optimize Nitrogen Fate in Paddy Soils. *Agriculture* **2024**, *14*, 2300. [CrossRef]
53. Xu, X.; Xiao, C.; Bi, R.; Jiao, Y.; Wang, B.; Dong, Y.; Xiong, Z. Optimizing organic fertilization towards sustainable vegetable production evaluated by long-term field measurement and multi-level fuzzy comprehensive model. *Agric. Ecosyst. Environ.* **2024**, *368*, 109008. [CrossRef]
54. Zhang, Y.; Wang, F.; Zhang, J.; Zhu, T.; Lin, C.; Müller, C.; Cai, Z. Cattle manure and straw have contrasting effects on organic nitrogen mineralization pathways in a subtropical paddy soil. *Acta Agric. Scand. Sect. B—Soil Plant Sci.* **2015**, *65*, 619–628. [CrossRef]
55. Hao, X.; Zhou, B.; Ma, X.; Gao, Z. Characteristics of crop yield and nutrient balance under different long-term fertilization practices in black soil. *Trans. Chin. Soc. Agric. Eng.* **2015**, *31*, 178–185. [CrossRef]
56. Hao, X.-Y.; Ma, X.-Z.; Gao, Z.-C.; Zhou, B.-K. Variation Characteristics of Fractions of Active Nitrogen and Organic Nitrogen Under Different Long-Term Fertilization Practices in Black Soil. *Sci. Agric. Sin.* **2015**, *48*, 4707–4716.
57. Daunoras Jokūbas Kaergius, A.; Gudiukait, R. Role of Soil Microbiota Enzymes in Soil Health and Activity Changes Depending on Climate Change and the Type of Soil Ecosystem. *Biology* **2024**, *13*, 85. [CrossRef] [PubMed]

58. Wang, L.; Zhang, H.; Xu, C.; Yuan, J.; Xu, X.; Wang, J.; Zhang, Y. Long-term nitrogen fertilization and sweetpotato cultivation in the wheat-sweetpotato rotation system decrease alkaline phosphomonoesterase activity by regulating soil phoD-harboring bacteria communities. *Sci. Total Environ.* **2023**, *900*, 165916. [CrossRef] [PubMed]
59. Xu, W.; Zhang, Y.; Liu, W.; Zhao, C.; Tahir, A.; Yang, C.; Guo, X.; Sun, R.; Yan, X.; Yuan, H.; et al. Twelve-year organic substitution fertilization mitigates microbial nutrient limitation and enhances soil carbon pool stability in a rubber plantation. *Plant Soil* **2026**, *521*, 129–149. [CrossRef]
60. Tang, Y.; Yang, X.; Wang, X.; Du, G.; Soothar, M.K.; Tian, Q.; Qi, Y. Soil Inorganic Carbon Losses Counteracted Soil Organic Carbon Increases in Deeper Soil over 30 Years in North China. *Land* **2025**, *14*, 1616. [CrossRef]
61. Zhang, F.; Chen, M.R.; Xing, Y.Y.; Wang, X. Appropriate nitrogen application under ridge-furrow plastic film mulching planting optimizes spring maize growth characteristics by improving soil quality in the Loess Plateau of China. *Agric. Water Manag.* **2025**, *307*, 109259. [CrossRef]
62. Zhang, Q.; Yan, S.; Zhang, X.; Ji, T.; Song, Q.; Yan, C.; Ma, C.; Gong, Z. Straw Incorporation Thresholds for Soil Carbon and Nitrogen Stability in Maize Cropping and Fallow Systems. *Eur. J. Soil Sci.* **2026**, *77*, e70312. [CrossRef]

Disclaimer/Publisher's Note: The statements, opinions and data contained in all publications are solely those of the individual author(s) and contributor(s) and not of MDPI and/or the editor(s). MDPI and/or the editor(s) disclaim responsibility for any injury to people or property resulting from any ideas, methods, instructions or products referred to in the content.